Chaos and quantum Fisher information in the quantum kicked top*

Wang Xiao-Qian(王晓茜)[a)b)], Ma Jian(马 健)[b)],
Zhang Xi-He(张喜和)[a)], and Wang Xiao-Guang(王晓光)[b)†]

[a)] *Department of Physics, Changchun University of Science and Technology, Changchun* 130022, *China*
[b)] *Zhejiang Institute of Modern Physics, Department of Physics, Zhejiang University, Hangzhou* 310027, *China*

(Received 28 September 2010; revised manuscript received 9 December 2010)

Quantum Fisher information is related to the problem of parameter estimation. Recently, a criterion has been proposed for entanglement in multipartite systems based on quantum Fisher information. This paper studies the behaviours of quantum Fisher information in the quantum kicked top model, whose classical correspondence can be chaotic. It finds that, first, detected by quantum Fisher information, the quantum kicked top is entangled whether the system is in chaotic or in regular case. Secondly, the quantum Fisher information is larger in chaotic case than that in regular case, which means, the system is more sensitive in the chaotic case.

Keywords: quantum information, quantum kicked top, quantum Fisher information, quantum chaos

PACS: 05.45.Mt, 03.65.Ud, 06.20.Dk **DOI:** 10.1088/1674-1056/20/5/050510

1. Introduction

In the field of quantum chaos,[1−3] the central problem is to study the special properties of a quantum system when its classical correspondent is chaotic. Some concepts have been used to characterize quantum chaos, such as decoherence,[4,5] sensitivity to perturbations,[6−8] fidelity decay,[9−11] and entanglement.[9,12−26] Spin squeezing is a useful tool to detect the quantum entanglement and the spin squeezing parameters can be used as entanglement witnesses.[26−37] The definitions of spin squeezing parameters are not unique and there are two most popular spin squeezing parameters. The first spin squeezing parameter, introduced by Kitagawa and Ueda,[30] is related to pairwise entanglement and in Refs. [18] and [21], the authors mainly study the properties of this spin squeezing parameter in quantum kicked top (QKT) model and Dicke model. The authors consider the initial states as coherent spin states, at the early period the states turn to be spin squeezed. As time goes on, the states become non-squeezed when the initial states are in the chaotic region, while the states will be squeezed for a considerable long time when the initial states are in the regular region. The second spin squeezing parameter, introduced by Wineland *et al.*,[29] is related to multipartite entanglement. In the following discussions, we use this parameter to describe the spin squeezing and multipartite entanglement.

Errors of quantum measurement are inevitable, thus it is useful to study the characters of sensitivity to measurement errors. Quantum Fisher information (QFI)[38−43] provides a fundamental limit above which the quantum states can be distinguished by measurement. In Ref. [43], the authors found that the QFI provides both a criterion for multipartite entanglement and a necessary and sufficient condition for shot-noise phase estimation. The authors also found that the criterion of entanglement given by QFI is stronger than that given by spin squeezing parameter.

The QKT model is a typical model to investigate quantum chaos,[16−18,44−47] and the entanglement, described by concurrence and entropy, can indicate the presence of quantum chaos.[16−18,47] In Ref. [47], the authors provide experimental proof that entanglement and sensitivity to perturbation can be taken as a quantum signature of chaos in the QKT model. In this paper, we study the evolutions of the QFI in the QKT model. We find that, the behaviours of the QFI are strongly influenced by quantum chaos. When the initial state is in regular region, the evolution of the QFI exhibits quasi-periodic behaviour, while when the initial state is in the chaotic region, the evolution becomes irregular. By using the QFI to characterize the

*Project supported by National Natural Science Foundation of China (Grant Nos. 11025527, 10874151, and 10935010).
†Corresponding author. E-mail: xgwang@zimp.zju.edu.cn
© 2011 Chinese Physical Society and IOP Publishing Ltd

entanglement of the QKT model, we find that the system is entangled whether the initial state is located in chaotic or in regular region and the result coincides with that given by linear entropy. By using the QFI to characterize the phase estimation, we can find that the phase sensitivity of this system in the chaotic case is stronger than that in the regular case.

The paper is organized as follows: In Section 2, we introduce the QKT model and describe its classical correspondent. In Section 3, we study the evolution of the QFI in the QKT model whose classical correspondent is chaotic. The conclusions are finally given in Section 4.

2. Quantum kicked top

The Hamiltonian of the QKT can be written as[44−46]

$$H = \frac{\hbar\kappa}{2j\tau}J_z^2 + \hbar p J_y \sum_{n=-\infty}^{\infty}\delta(t-n\tau), \tag{1}$$

where J_i ($i \in \{x, y, z\}$) are angular momentum operators and the magnitude $J^2 = j(j+1)\hbar^2$, τ is the periodic time between kicks and without loss of generality, we set $\tau = 1$ in the following. The first term in Eq. (1) describes a nonlinear precession around the z-axis of strength κ. The second term describes periodic kicks, which corresponds to a rotation about the y-axis. The kicked term is applied at time intervals of $n\tau$ with strength p. We turn to the Heisenberg picture, the expectation values of the angular momentum operators can be written as $\langle J_i\rangle_{n+1} = \langle U^\dagger J_i U\rangle_n$, where U is the Floquet operator describing the unitary evolution for each kick,

$$U = \exp\left(-\mathrm{i}\,\frac{\kappa}{2j}J_z^2\right)\exp(-\mathrm{i}\,pJ_y) \tag{2}$$

with $\hbar = 1$.

The QKT shows chaotic dynamics in the classical limit as $j \to \infty$.[44−46] The expressions for the components of angular momentum are given as $X = \langle J_x/j\rangle$, $Y = \langle J_y/j\rangle$ and $Z = \langle J_z/j\rangle$. For the special case of $p = \pi/2$, we have the classical equations of motion[44−46]

$$\begin{bmatrix} X' \\ Y' \\ Z' \end{bmatrix} = \begin{bmatrix} Z\cos(\kappa X) + Y\sin(\kappa X) \\ -Z\sin(\kappa X) + Y\cos(\kappa X) \\ -X \end{bmatrix}, \tag{3}$$

the variables $\{X, Y, Z\}$ obey the relation $X^2 + Y^2 + Z^2 = 1$ and can be written as

$$(X, Y, Z) = (\sin\theta\cos\phi, \sin\theta\sin\phi, \cos\theta) \tag{4}$$

in polar coordinates, θ is the polar angle and ϕ is the azimuthal angle. Thus, the transformation gives a two-dimensional map. From Refs. [16] and [17], for small values of κ, the classical phase space is dominated by islands of regular (periodic) motions, which is destroyed as the κ increases. For $\kappa = 3$, the phase space becomes mixed with regular and chaotic regions and we show the stroboscopic phase space map of the QKT with $\kappa = 3$ in Fig. 1. To study the dynamic behaviours of the system, we should choose the initial states centred in both regular and chaotic regions of the corresponding classical phase space. From Fig. 1, we find that the point $(\theta, \phi) = (2.25, -2.2)$ is in the critical region and then we consider the classical characteristic of the critical region. We plot the evolution of the classical equations of motion for different κ with $\theta = 2.25, \phi = -2.2$, from Fig. 2, we find that there are bifurcations for the angles θ and ϕ. When $\kappa = 3$, there are two stable points, namely, the initial state whose classical correspondent is in the period-two region and the period-two region can be viewed as regular region.

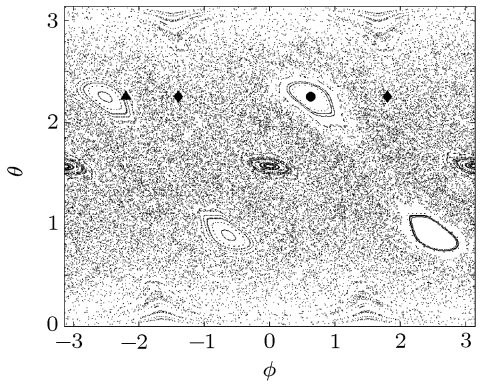


Fig. 1. Stroboscopic phase-space dynamics of the classical kicked top for $\kappa = 3$. There are 200 initial states, distributed randomly in the phase space, each evolves for 200 kicked. The marks represent the various choices for the initial states: a circle at $(\theta, \phi) = (2.25, 0.63)$ is just the fixed point; a triangle at $(\theta, \phi) = (2.25, -2.2)$ is in the critical region; two diamonds at $(\theta, \phi) = (2.25, 1.8)$ and $(\theta, \phi) = (2.25, -1.4)$ are in the chaotic region.

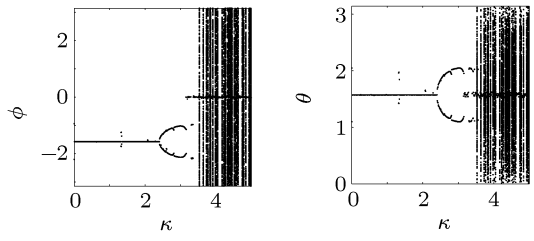


Fig. 2. Bifurcation diagrams for the classical phase-space at $\theta = 2.25, \phi = -2.2$ with different κ. When $\kappa = 3$, there are two fixed points, namely, the state is in the period-two region.

3. Quantum Fisher information

The QFI is a fundamental of estimation theory in statistics.[38−43] We consider a quantum state denoted by $\rho(\varphi)$, which is supposed to depend on an unknown parameter φ. Consider a measurement to realize the system, no matter how to design the method to measure the system, there is an unavoidable error associated with the measurement. The variance of φ is limited by quantum Cramér–Rao lower bound

$$(\delta\varphi)^2 \geq \Delta\varphi_{\mathrm{QCR}} = \frac{1}{F[\rho(\varphi)]} \tag{5}$$

with $F[\rho(\varphi)]$ the QFI, given by

$$F[\rho(\varphi)] = \mathrm{tr}\left[\rho(\varphi) L_\varphi^2\right], \tag{6}$$

where L_φ is the so-called symmetry-logarithm derivative (SLD), given by

$$\partial_\varphi \rho(\varphi) = \frac{1}{2}\left[L_\varphi \rho(\varphi) + \rho(\varphi) L_\varphi\right]. \tag{7}$$

When $\rho(\varphi)$ is a pure state, it is generated by the following rotation:

$$\rho(\varphi) = \mathrm{e}^{-\mathrm{i}\varphi J_{\boldsymbol{n}}} \rho \mathrm{e}^{\mathrm{i}\varphi J_{\boldsymbol{n}}}, \tag{8}$$

where $J_{\boldsymbol{n}} = \boldsymbol{J}\cdot\boldsymbol{n}$, we have $F[\rho(\varphi)] = 4\mathrm{tr}\left[\rho(\varphi) J_{\boldsymbol{n}}^2\right] = 4(\Delta J_{\boldsymbol{n}})^2$, since $\mathrm{tr}[\rho(\varphi) J_{\boldsymbol{n}}] = 0$. In Ref. [43], the authors give a sufficient condition for multipartite entanglement by using the QFI

$$\chi^2 \equiv \frac{N}{F[\rho(\varphi)]} < 1. \tag{9}$$

We consider the spin squeezing parameter defined by Wineland *et al.*,[29]

$$\xi^2 = \frac{N(\Delta J_{\boldsymbol{n}_\perp})^2}{|\langle \boldsymbol{J}\cdot\boldsymbol{n}\rangle|^2}, \tag{10}$$

where $N = 2j$ is the total number of qubits and the subscript $\boldsymbol{n}_\perp$ is the axis perpendicular to the mean spin direction $\boldsymbol{n} = \langle \boldsymbol{J}\rangle / |\langle \boldsymbol{J}\rangle|$. When the state satisfies the inequality $\xi^2 < 1$, the system is entangled[14] and spin squeezed.[29,30] From the uncertainty relation

$$(\Delta J_{\boldsymbol{n}_1})^2 (\Delta J_{\boldsymbol{n}_2})^2 \geq \frac{1}{4}\langle J_{\boldsymbol{n}_3}\rangle^2, \tag{11}$$

we obtain

$$\chi^2 = \frac{N}{4(\Delta J_{\boldsymbol{n}_1})^2} \leq \frac{N(\Delta J_{\boldsymbol{n}_2})^2}{\langle J_{\boldsymbol{n}_3}\rangle^2} = \xi^2. \tag{12}$$

Therefore, the new criterion for particle entanglement $\chi^2 < 1$ is stronger than the spin squeezing condition $\xi^2 < 1$. For the reason that the QFI can be stronger described by the entanglement of quantum system than spin squeezing and the QFI provides the ultimate limits for parameter estimation, we can study the properties of the QFI in the quantum chaos. To connect the quantum and classical dynamics of the QKT,[44−46] we start with the coherence spin state (CSS), whose centre is a point in the classical phase-space, the CSS is defined as

$$|\,\theta,\phi\rangle = R(\theta,\phi)|j,j\rangle, \tag{13}$$

where $-\pi \leq \theta \leq \pi, 0 \leq \phi \leq \pi$; $|j,j\rangle$ is the eigenstate of J_z, with the eigenvalue j. The rotation operator is defined as

$$R(\theta,\phi) = \exp\{\mathrm{i}\,\theta[J_x\sin\phi - J_y\cos\phi]\}. \tag{14}$$

The expectation value of the angular momenta in this state is given by $\langle \boldsymbol{J}\rangle = (J_x, J_y, J_z) = j(\sin\theta\cos\phi, \sin\theta\sin\phi, \cos\theta)$. The evolution is controlled by the unitary operator U, the state vector at step n is given by

$$|\psi(n)\rangle = U^n|\theta,\phi\rangle, \tag{15}$$

where U is defined in Eq. (2).

For quantum measurement, there are the shot-noise limit, where the uncertainty scales as $1/\sqrt{N}$ and the Heisenberg limit, where the uncertainty scales as $1/N$. In Ref. [43], $\chi^2 < 1$ is not only a sufficient condition for particle entanglement, but also a condition for shot-noise phase estimation sensitivity. In Fig. 3, we plot the evolution of the QFI with different initial states. We find that no matter which region the initial state is in, χ^2 is always smaller than 1 after the first kick. It means that in the QKT system, after the first kick, the state is entangled. When the initial state is at the fixed point, the evolution of χ^2 shows periodic behaviour [Fig. 3(a)]. When the initial state is in the period-two region, the evolution of χ^2 shows quasi-periodic behaviour [Fig. 3(b)]. We can find that the evolutions of χ^2 are declined at first in the regular case and it takes a relatively long time for χ^2 to obtain the minimal value in the regular case and the minimal value persists a short time. Comparing Fig. 3(a) with Fig. 3(b), when the initial state is at the fixed point, the minimal value of χ^2 is smaller than that in the period-two region, on the contrary, the existed time of the minimal value in the period-two region is longer than that at the fixed point. When the initial states are in the chaotic region, as shown in Figs. 3(c) and 3(d), the evolutions of χ^2 become irregular and the curves are declined at first and rapidly reduced to a small value. Here we give the average value of χ^2 with different initial states, as shown in Fig. 4. Comparing Fig. 4 with Fig. 1, we can find that the average value

of χ^2 is larger in the regular region than that in the chaotic region. By studying QFI, we find a very good quantum-classical correspondence.

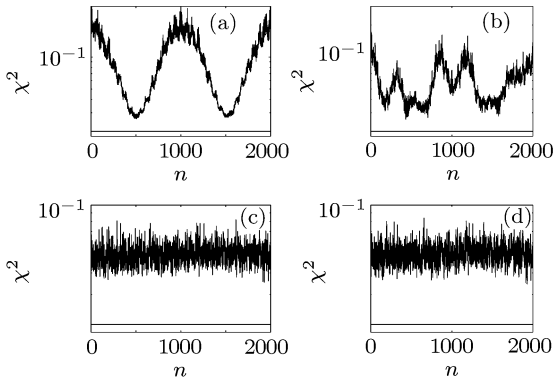


Fig. 3. Evolution of χ^2 with different initial CSSs. The horizontal line is the Heisenberg limit, here we choose $N = 50$, (a) $\theta = 2.25$, $\phi = 0.63$ (at the fixed point); (b) $\theta = 2.25$, $\phi = -2.2$ (in the period two region); (c) $\theta = 2.25$, $\phi = 1.8$ (in the chaotic region); (d) $\theta = 2.25$, $\phi = -1.4$ (in the chaotic region).

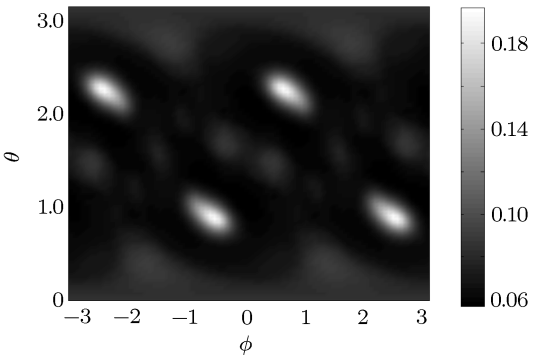


Fig. 4. Average value of χ^2 with 1000 kicks in the classical phase space and $N = 50$. Comparing with Fig. 1, we can see that there are very obvious relations between χ^2 and the classical dynamics of the system. The χ^2 in the regular regions are larger than that in the chaotic regions.

To determine whether a state is entangled, we just need to measure the collective operators, which are particle populations in many cases. Thus, spin squeezing parameter is a useful tool to detect entanglement. The spin squeezing parameter ξ^2 is the ratio of the fluctuations between a general state and a CSS in the determination of the resonance frequency in Ramsey spectroscopy. Thus, this parameter is associated with improvement of measurement precision. References [26]–[28] proved that a many-body system is entangled when $\xi^2 < 1$. Spin squeezing is very sensitive to the quantum chaos.[21] We compare spin squeezing parameter ξ^2 with the QFI in Fig. 5. If we consider the spin squeezing parameter, the classical chaos suppresses the spin squeezing[21] and enhances the entanglement quantified by the linear entropy.[13] Thus, we can say that the spin squeezing parameter ξ^2 is smaller than 1, the system is entangled, but the converse is not hold. Here, we consider χ^2 in this system, no matter which region the initial state is in, χ^2 is always smaller than 1, implying that the system displays entanglement. Thus, the QFI describing the entanglement coincides with the linear entropy. In Fig. 5, we plot the evolution of the uncertainty, the system always satisfies the uncertainty relation.

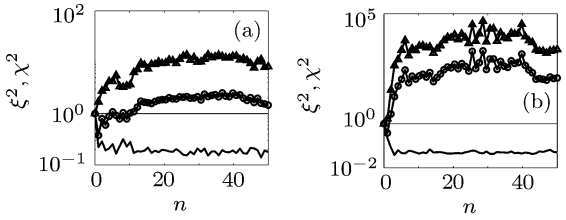


Fig. 5. Evolution over time of spin squeezing parameter ξ^2 (circles) and χ^2 (solid line) with different initial CSS. Here we choose $N = 50$, the triangles are plotted for the uncertainty relation $\xi^2/\chi^2 \geq 1$, (a) $\theta = 2.25, \phi = 0.63$ (at the fixed point); (b) $\theta = 2.25, \phi = 1.8$ (in the chaotic regions).

In the following, we consider the average values of χ^2 for different N , whose initial states are in the regular and chaotic regions. If we choose the initial state located at $\theta = 2.25, \phi = 1.8$, whose classical correspondent is in the chaotic region, we plot the average values of χ^2 with different N on a log–log scale, displayed in Fig. 6.

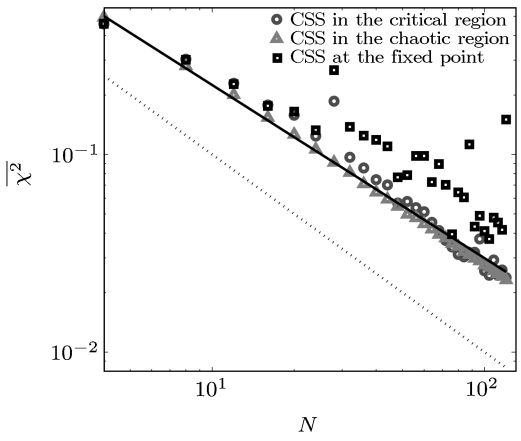


Fig. 6. Average value of χ^2 with 100 kicks for different N with the initial states in the chaotic and regular region. The initial states in the critical regions are denoted by circles and triangles denote those in the chaotic regions, squares denote those the fixed point. The solid line is the numerical fitting for the chaotic data. The Heisenberg limit is denoted by the dashed line.

We attempt to fit these datum by a straight line representing a linear relation as $\chi^2 \sim N^{-0.8759}$ and then the QCR bound as $\Delta\varphi_{\rm QCR} \sim N^{-0.938}$, which approaches the Heisenberg limit N^{-1}. When the initial states are in the regular regions, as shown in Fig. 6,

the sensitivity of the QKT system is not as well as that in the chaotic region. In general with the same N, the average values of χ^2 in the regular case are larger than those in the chaotic case. And the average values of χ^2 are the largest when the initial state is at the fixed point and the smallest in the chaotic region, namely, the system is more chaotic, it is more sensitive in phase estimation.

4. Conclusion

In this paper, we study the QFI in the QKT model whose classical correspondent exhibits the chaotic and regular behaviours, we find that the QFI strongly influences the quantum chaos. According to the average values of χ^2, the system is more sensitive in phase estimation when the initial states are in the chaotic region. We have found that the QFI can well describe the quantum chaos. The $\chi^2 < 1$ can be viewed as a criterion of quantum entanglement, the system displays entanglement both in the chaotic and in the regular cases. For the evolutions of χ^2, when the initial states are in the chaotic region, the evolutions of χ^2 are declined quickly. Thus for the phase estimation, the system in the chaotic region is more useful than that in the regular region. Consider the average value of χ^2 with respect to kicked times for different Ns, we can find that if the initial CSS is in the chaotic region, the QCR bound of this system approaches the Heisenberg limit. We believe that similar results may also be found in other models that exhibited quantum chaos, e.g. the Dicke model.

References

[1] Gutzwiller M C 1990 *Chaos in Classical and Quantum Mechanics* (New York: Springer-Verlag) p. 173
[2] Stöckmann H J 1999 *Quantum Chaos: An Introduction* (Cambridge: Cambridge University Press) p. 246
[3] Peres A 1984 *Phys. Rev.* A **30** 1610
[4] Fried H M, Gabellini Y and McKellar B H 1995 *Phys. Rev. Lett.* **74** 4373
[5] Jalabert R A and Pastawski H M 2001 *Phys. Rev. Lett.* **86** 2490
[6] Schack R and Caves C M 1996 *Phys. Rev.* E **53** 3257
[7] Breslin J K and Milburn G J 1999 *Phys. Rev.* A **59** 1781
[8] Liu X M, Hug M and Milburn G J 2000 *Phys. Rev.* A **62** 043801
[9] Gorin T, Prosen T, Selingman T H and Žnidarič M 2006 *Phys. Rep.* **435** 33
[10] Emerson J, Weinstein Y S, Lloyd S and Cory D G 2002 *Phys. Rev. Lett.* **89** 284102
[11] Weinstein Y S and Hellberg C S 2005 *Phys. Rev.* E **71** 016209
[12] Jacquod Ph 2004 *Phys. Rev. Lett.* **92** 150403
[13] Wang X, Ghose S, Sanders B C and Hu B 2004 *Phys. Rev.* E **70** 016217
[14] Wang X and Sanders B C 2003 *Phys. Rev.* A **68** 033821
[15] Weinstein Y S and Viola L 2006 *Europhys. Lett.* **76** 746
[16] Ghose S, Stock R, Jessen P, Lal R and Silberfarb A 2008 *Phys. Rev.* A **78** 042318
[17] Stamatiou G and Ghikas D P K 2007 *Phys. Lett.* A **368** 206
[18] Song L, Wang X, Yan D and Zong Z 2006 *J. Phys.* B: *At. Mol. Opt. Phys.* **39** 559
[19] Furuya K, Nemes M C and Pellegrino G Q 1998 *Phys. Rev. Lett.* **80** 5524
[20] Petijean C and Jacquod Ph 2006 *Phys. Rev. Lett.* **97** 194103
[21] Song L, Yan D, Ma J and Wang X 2009 *Phys. Rev.* E **79,** 046220
[22] Song L, Wang X, Li Y and Zong Z 2006 *Chin. Phys. Lett.* **23** 3190
[23] Song L, Yan D, Gai Y and Wang Y 2010 *Acta Phys. Sin.* **59** 3695 (in Chinese)
[24] Yan D and Song L 2010 *Acta Phys. Sin.* **59** 6832 (in Chinese)
[25] Zhou L, Song H and Yao L 2001 *Chin. Phys.* **10** 413
[26] Sørensen A S, Duan L M, Cirac J I and Zoller P 2001 *Nature* **409** 63
[27] Sørensen A S 2002 *Phys. Rev.* A **65** 043610
[28] Sørensen A S and Mølmer K 2001 *Phys. Rev. Lett.* **86** 4431
[29] Wineland D J, Bollinger J J, Itano W M and Heinzen D J 1994 *Phys. Rev.* A **50** 67
[30] Kitagawa M and Ueda M 1993 *Phys. Rev.* A **47** 5138
[31] Tóth G, Knapp C, Gühne O and Briegel H J 2009 *Phys. Rev.* A **79** 042334
[32] Alekseev K N and Priĭmak D S 1998 *JETP* **86** 61
[33] Alekseev K N 1995 *Opt. Commun.* **116** 468
[34] Alekseev K N and Perina J 1998 *Phys. Rev.* E **57** 4023
[35] Alekseev K N and Peřina J 1997 *Phys. Lett.* A **231** 373
[36] Pu H, Zhang W and Meystre P 2002 *Phys. Rev. Lett.* **89** 090401
[37] Raghavan S, Pu H, Meystre P and Bigelow N P 2001 *Opt. Commun.* **188** 149
[38] Weiss C and Teichmann N 2009 *J. Phys.* B: *At. Mol. Opt. Phys.* **42** 031001
[39] Hall M J W 2000 *Phys. Rev.* A **62** 012107
[40] Barndorff-Nielsen O E and Gill R D 2000 *J. Phys.* A: *Math. Gen.* **33** 4481
[41] Gibilisco P and Isola T 2007 *AISM* **59** 147
[42] Helstrom C W 1976 *Quantum Detection and Estimation Theory* (New York: Academic Press) p. 235
[43] Pezzé L and Smerzi A 2009 *Phys. Rev. Lett.* **102** 100401
[44] Arecchi F T, Courtens E, Gilmore R and Thomas H 1972 *Phys. Rev.* A **6** 2211
[45] Haake F, Kuś M and Scharf R 1987 *Z. Phys.* B-*Condensed Matter* **65** 381
[46] D'Ariano G M, Evangelista L R and Saraceno M 1992 *Phys. Rev.* A **45** 3646
[47] Chaudhury S, Smith A anderson B E, Ghose S and Jessen P S 2009 *Nature* **461** 768